High-Density Lipoprotein Transport Through Aortic Endothelial Cells Involves Scavenger Receptor BI and ATP-Binding Cassette Transporter G1

Lucia Rohrer, Pascale M. Ohnsorg, Marc Lehner, Franziska Landolt, Franz Rinninger, Arnold von Eckardstein

Abstract—Cholesterol efflux from macrophage foam cells is a rate-limiting step in reverse cholesterol transport. In this process cholesterol acceptors like high-density lipoproteins (HDL) and apolipoprotein (apo)A-I must cross the endothelium to get access to the donor cells in the arterial intima. Previously, we have shown that apoA-I passes a monolayer of aortic endothelial cells (ECs) from the apical to the basolateral side by transcytosis, which is modulated by the ATP-binding cassette transporter (ABC)A1. Here, we analyzed the interaction of mature HDL with ECs. ECs bind HDL in a specific and saturable manner. Both cell surface biotinylation experiments and immunofluorescence microscopy of HDL recovered ≈30% of the cell-associated HDL intracellularly. Cultivated on inserts ECs bind, internalize, and translocate HDL from the apical to the basolateral compartment in a specific and temperature-dependent manner. The size of the translocated particle was reduced, but its protein moiety remained intact. Using RNA interference, we investigated the impact of SR-BI, ABCA1, and ABCG1 on binding, internalization, and transcytosis of HDL by ECs. HDL binding was reduced by 50% and 30% after silencing of SR-BI and ABCG1, respectively, but not at all after diminishing ABCA1 expression. Knock down of SR-BI and, even more so, ABCG1 reduced HDL transcytosis but did not affect inulin permeability. Cosilencing of both proteins did not further reduce HDL binding, internalization, or transport. In conclusion, ECs transcytose HDL by mechanisms that involve either SR-BI or ABCG1 but not ABCA1. **(*Circ Res*. 2009;104:1142-1150.)**

Key Words: cholesterol homeostasis ■ endothelial cells ■ lipoproteins ■ vascular endothelial function ■ vascular permeability

Plasma concentrations of high-density lipoprotein (HDL) cholesterol show an inverse association with the incidence of coronary artery disease. The cardioprotective effect of HDL and its major apolipoprotein (apo)A-I are, in part, related to the ability to promote the reverse transport of cholesterol from macrophage foam cells in the arterial intima to the liver for excretion into the bile.[1–4] An early step in the reverse transport of cholesterol is the transfer of excess cholesterol from the lipid-laden macrophages to HDLs. Importantly, the loading of cellular cholesterol to HDL does not take place in the plasma compartment but in the subendothelial space of arteries.[1] Consequently, HDLs must cross the endothelium to get into close proximity to the cholesterol donor cells. This passage is not well understood.[5]

The endothelium lines the vasculature as a single layer of endothelial cells (ECs). As a semipermeable barrier, it regulates the flux of liquid, solutes, and cells between blood and interstitial space. Two principal pathways are known for transendothelial macromolecule translocation, the transcellular transport, including transcytosis, and the paracellular transfer between adjacent cells.[6,7] The paracellular pathway is formed by gaps between ECs, but regulated adherence and tight junctions restrict and control the free passage of macromolecules larger than 6 nm.[7] Endothelial transcytosis, which is defined as vesicle-mediated transport of proteins, has been best investigated for albumin.[8] Recently, we have shown that ECs bind, internalize, and transport lipid-free apoA-I in a specific manner. The transcellular transport of apoA-I is temperature-dependent, involves the ATP-binding cassette transporter (ABC)A1, and generates a lipidated particle.[9,10]

In the plasma, the majority of apoA-I is lipid-bound and assembled in spherical HDL. We hypothesized that spherical HDL crosses the endothelium similar to lipid-free apoA-I and therefore investigated binding, uptake, and transport of HDL by cultured aortic ECs and the involvement of the ATP-

Original received November 2, 2008; revision received March 28, 2009; accepted April 2, 2009.

From the Institute of Clinical Chemistry (L.R., P.M.O., M.L., F.L., A.v.E.), Center for Integrative Human Biology and Competence Center of Systems Physiology and Metabolic Diseases, University of Zurich, University Hospital Zurich, Switzerland; and University Hospital Hamburg Eppendorf (F.R.), Germany.

Correspondence to Lucia Rohrer, Institute of Clinical Chemistry, University Hospital Zurich, Rämistrasse 100, 8091 Zurich, Switzerland. E-mail lucia.rohrer@usz.ch

Circulation Research **is available at http://circres.ahajournals.org** **DOI: 10.1161/CIRCRESAHA.108.190587**

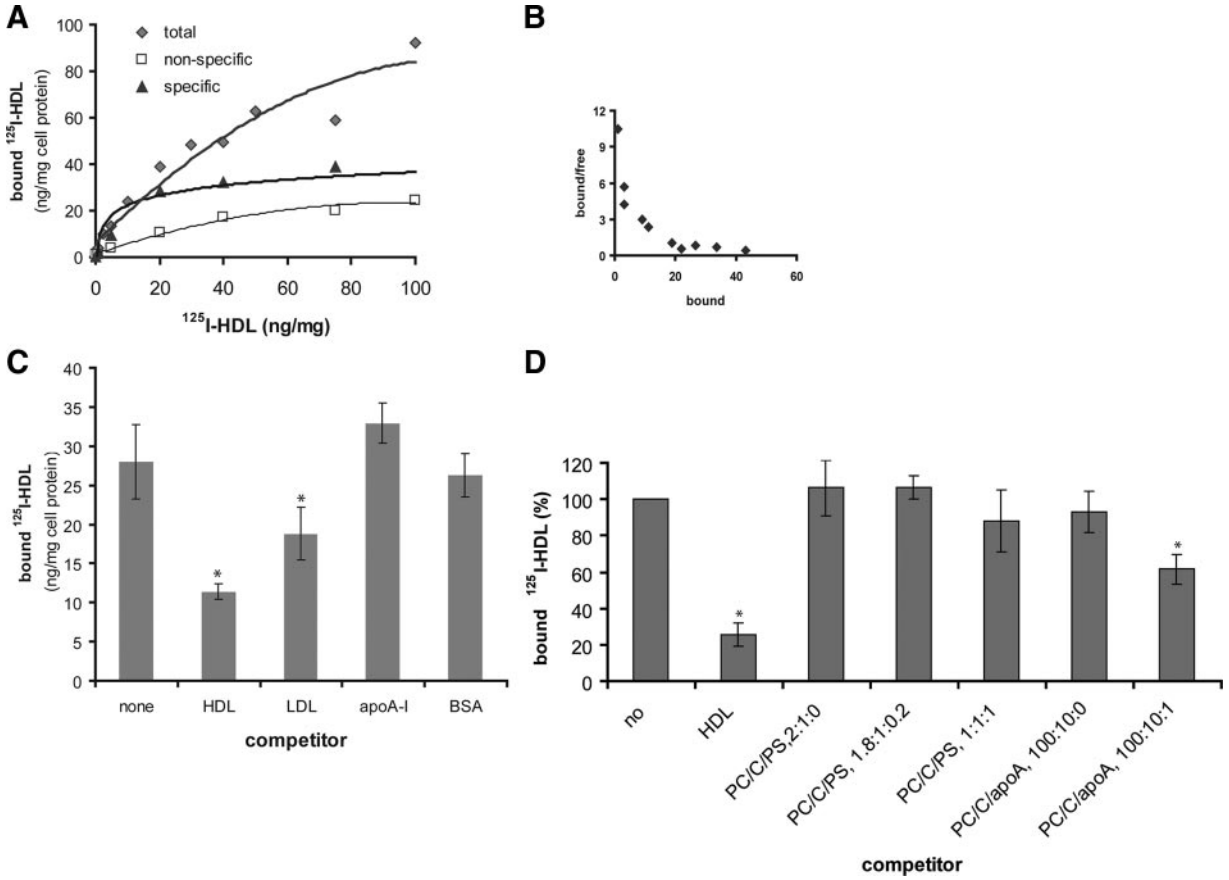

Figure 1. ^{125}I-HDL binding (4°C) to ECs is concentration-dependent (A) and specific (C). A, ECs were incubated at 4°C with the indicated concentration of ^{125}I-HDL in the absence (total) (◇) or in the presence of a 40-fold excess of unlabeled HDL (nonspecific) (□). Specific binding (▲) was calculated by subtracting the values of the unspecific binding from those of the total binding. B, Scatchard plot analysis reveals an easier reading of the equilibrium constants obtained after global fitting. C, To study specificity of binding, cells were incubated with 10 μg/mL ^{125}I-HDL in the absence or presence of 400 μg/mL the indicated competitor. D, The HDL-binding specificity was further evaluated with competition studies with liposomes of different lipid composition (400 μg/mL phospholipid: phosphatidylcholine [PC], phosphatidylserine [PS], cholesterol [C]). The results are represented as means±SD of at least 3 individual experiments. *$P<0.05$ vs control.

binding cassette transporters ABCA1 and ABCG1, as well as the HDL receptor scavenger receptor (SR)-BI.

Materials and Methods

Lipoproteins and Cells

Aortic ECs were isolated from bovine aorta and cultured in DMEM (Sigma) supplemented with 5% FCS (medium A) as described previously.[10]

Plasma HDL ($1.063<d<1.21$ g/mL) were isolated from fresh normolipidemic human plasma of blood donors by sequential ultracentrifugation as described previously.[9,10] HDL was iodinated with Na^{125}I by the McFarlane monochloride procedure as modified for lipoproteins.[11] Specific activities of approximately 300 to 700 cpm/ng protein were obtained.

Liposome preparations are described in the expanded Materials and Methods section, available in the online data supplement at http://circres.ahajournals.org.

Interactions of ^{125}I-HDL With Endothelial Cells

Binding, cell association, degradation, internalization, and transport of ^{125}I-HDL were assayed, in principle, as described previously for ^{125}I-apoA-I[10] (see the online data supplement).

Small Interfering RNA Transfection

ECs were transfected with 30 nmol/L BLOCK-iT fluorescent oligo and 100 nmol/L Stealth small interfering (si)RNA (Invitrogen) or 100 nmol/L siRNA siGenome ON-TARGETplus SMARTpool duplex (Dharmacon) against either SR-BI, ABCG1, or scrambled as described in the online data supplement.

Quantitative RT-PCR

RNA quantitative PCR was performed as described in the online data supplement.

Protein Analyses

Western blotting and gel filtration were performed as described in the online data supplement.

Results

HDL Interaction With Aortic Endothelial Cells

At first, the interaction of HDL with ECs was characterized as binding at 4°C, cell association at 37°C, internalization, degradation, and transport. The binding capacity of ECs for HDL was analyzed by using ^{125}I-HDL. Specific binding was calculated by subtracting from the values of the total binding those of the nonspecific binding, which is measured in the presence of a 40-fold excess of unlabeled HDL (Figure 1A). Binding was largely competed with a 40-fold excess of unlabeled HDL and to a much lesser degree but still signif-

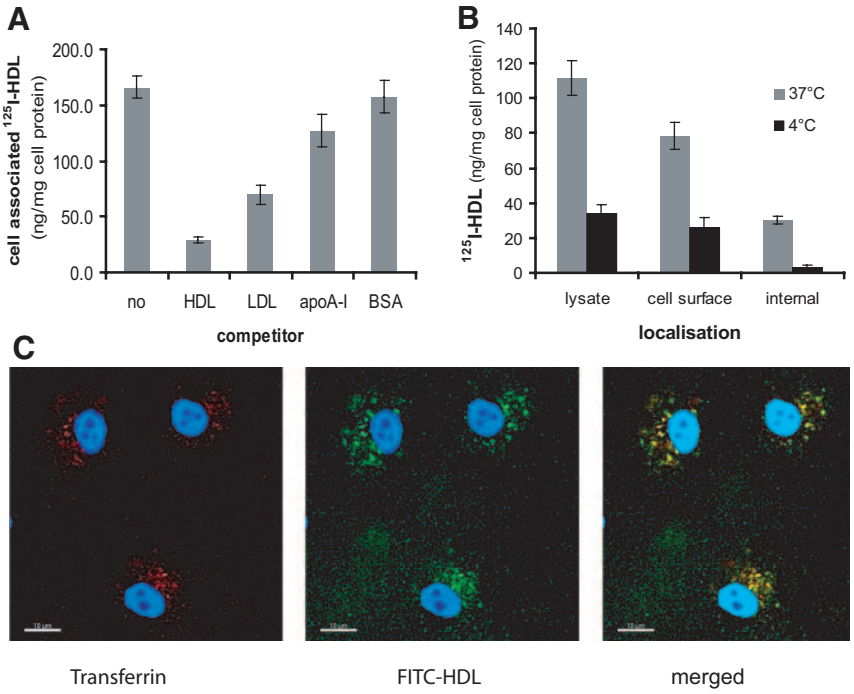

Figure 2. HDL cell association (37°C) and internalization to ECs. A, To study the specificity of the cell association, ECs were incubated with 10 μg/mL ^{125}I-HDL in the absence or presence of 400 μg/mL the indicated competitor. B, Repartition of specifically cell-associated (37°C) and the bound (4°C) ^{125}I-HDL as cell surface–bound and internal. C, The FITC-HDL internalization was analyzed by confocal fluorescent microscopy. ECs were incubated with FITC-HDL (green), together with Alexa 594–transferrin (red), and partial colocalizations (yellow) were assessed. The results are represented as means±SD of at least 3 individual experiments.

icantly with LDL but not at all with excess of lipid-free apoA-I and BSA (Figure 1C). Apolipoprotein-free liposomes of different lipid composition did not compete for HDL binding, but adding apoA-I into the liposomes partially restored the competition capacity (Figure 1D). These data argue for a specific receptor-mediated binding of HDL to ECs. ECs bound ^{125}I-HDL in a saturable manner. Scatchard plot analysis of the binding curve revealed multiple binding sites (Figure 1B), with B_{max} of 7.3±0.4 ng/mg for the high-affinity and B_{max} of 73.7±9.1 ng/mg for the low-affinity binding, respectively. Moreover, the K_d values were 1.2±0.4 μg/mL for high-affinity and 32.1±10.9 μg/mL for low-affinity binding (Figure 1B).

At 37°C, cell association was almost completely competed with a 40-fold excess of unlabeled HDL and partially competed with LDL but not at all with an excess of apoA-I or BSA (Figure 2A). The ^{125}I-HDL–specific cell association B_{max} values estimated from the Scatchard plot (data not shown) were 55.7±12.9 ng/mg for the high-affinity binding and 102±26 ng/mg for the low-affinity binding. In addition, the K_d values of HDL cell association (37°C) were similar to the K_d of binding (4°C) and amounted to 2.4±1.2 and 43.9±3.3 μg/mL for the high- and low-affinity sites, respectively.

Next, the cellular distribution of HDL was analyzed. Cell surface biotinylation experiments recovered ≈30% of the total cell-associated ^{125}I-HDL in intracellular compartments (Figure 2B). In contrast, at 4°C almost all ^{125}I-HDL bound to ECs was recovered on the surface, as expected. Internalization of HDL by ECs was further investigated by confocal fluorescence microscopy. ECs were incubated with FITC-HDL together with Alexa 594–transferrin. After 10 minutes of incubation, vesicles containing fluorescent HDL were partially colocalized with Alexa 594–transferrin (Figure 2C), confirming that HDL is internalized by ECs. The degradation

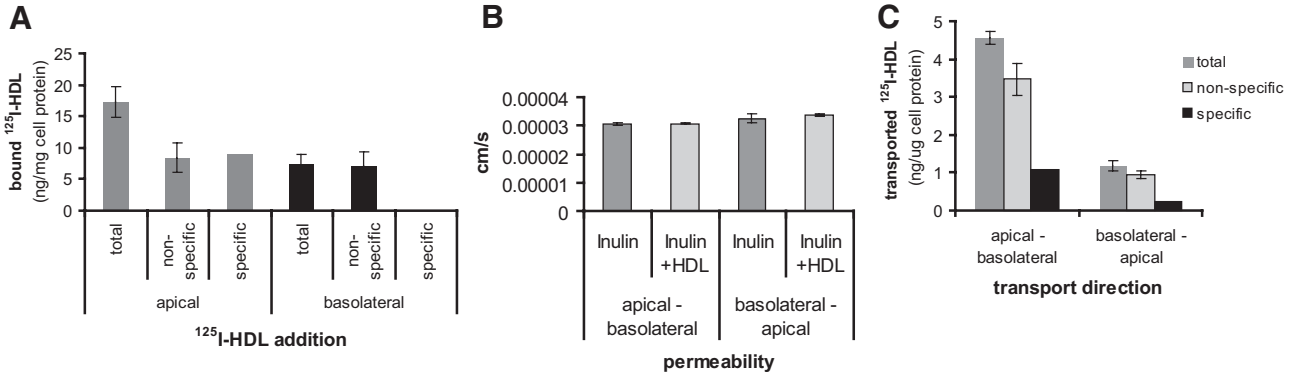

Figure 3. HDL binding to the apical and basolateral side and transport through a monolayer of ECs. A, ECs were cultured on inserts, and the binding of ^{125}I-HDL was measured by adding ^{125}I-HDL in the absence (total) or presence of 40-fold excess of unlabeled HDL (nonspecific), either into the apical or the basolateral compartment. B, The permeability of the EC monolayer to inulin was analyzed in both directions in the presence and absence of HDL. C, HDL transport from the apical to the basolateral compartment and in the opposite direction was measured. The results are represented as means±SD of at least 3 individual experiments.

of ^{125}I-HDL after 4 hours was measured as the release of radiolabeled degraded amino acids into the medium in the presence or absence of excess unlabeled HDL. The specific degradation was <5% of the specific cell association (data not shown).

Transport of HDL Through a Monolayer of Endothelial Cells

In the vessel wall, the ECs are polarized. To separately analyze the binding affinity of both apical and basolateral sides, we cultured the cells on porous membrane inserts to form a confluent and presumably polarized cell layer. The distribution of the HDL-binding sites in these cells was studied by adding the label either into the apical compartment or into the basolateral compartment. HDL bound specifically to the apical side, but no specific binding to the basolateral side of the cell layer was obtained (Figure 3A). To analyze the accessibility of the cell layer on the basolateral side, as well as the intactness of the barrier function, we measured the permeability coefficient of ^{3}H-inulin, which does not cross cell membranes and hence represents a paracellular transport marker. The tracer was added to the apical chamber, and the filtered radioactivity was measured in the basolateral compartment and vice versa. The permeability coefficients for ^{3}H-inulin across the EC layer were calculated over a time period of 1 hour and were similar for both directions, namely $3.06\pm0.22\times10^{-5}$ cm/sec and $3.25\pm0.03\times10^{-5}$ cm/sec for apical-to-basolateral and basolateral-to-apical transports, respectively. This indicates that the membrane did not hinder inulin diffusion from the basolateral to the apical compartment (Figure 3B). Furthermore, we assessed the influence of 30 μg/mL HDL in the donor compartment on the permeability of ^{3}H-inulin. The permeability coefficients of ^{3}H-inulin in the presence of HDL were similar, as described above, namely $3.07\pm0.2\times10^{-5}$ cm/sec and $3.31\pm0.02\times10^{-5}$ cm/sec for apical-to-basolateral and basolateral-to-apical transports, respectively, and not significantly different from the permeability coefficients of ^{3}H-inulin alone (Figure 3B). The data indicate that HDL does not change the barrier function of the monolayer.

With this model, we addressed the question of whether ECs transport HDL through the cell layer. At first, the transport direction of HDL in the insert was analyzed by adding the label in the presence of a 40-fold excess and in the absence of excess cold HDL into either the apical or the basolateral compartments of the cell culture system (Figure 3C). The appearance of ^{125}I-HDL in the opposite compartment was measured. We recorded specific apical-to-basolateral transport but no basolateral-to-apical transport (Figure 3C), whereas inulin permeability was similar in both directions (Figure 3B). This suggests that HDL is transported transcellularly through ECs from apical to basolateral. SDS-PAGE analysis of the radioactive material recovered in the basolateral compartment revealed that the protein moiety of HDL remained intact during transendothelial transport (Figure 4A). Interestingly, gel filtration analysis of the transported material showed a reduced size of the transported particle (Figure 4B). The Stokes diameter of the material harvested in the basolateral compartment after translocation through the EC layer

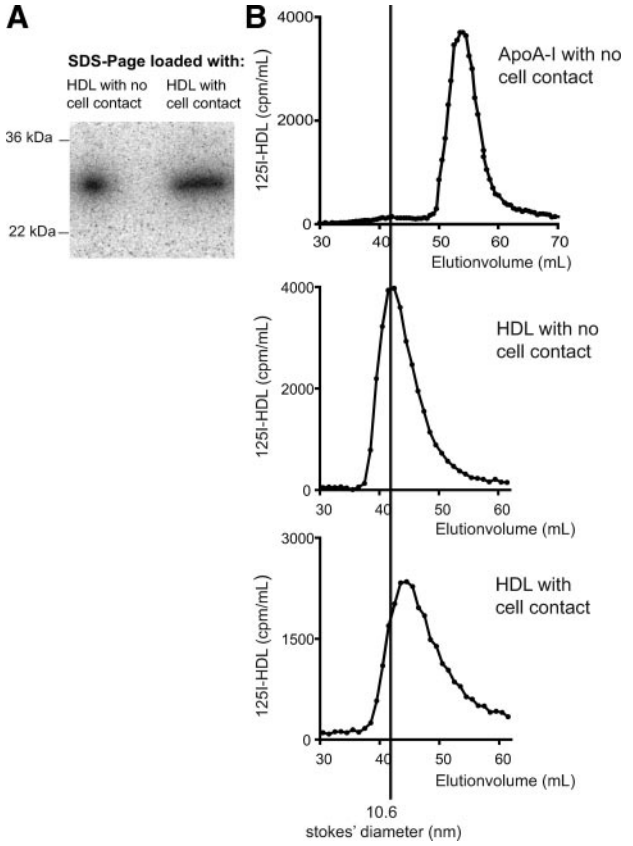

Figure 4. The particle size of the transported HDL is reduced, but the protein moiety remains intact. ^{125}I-HDL (30 μg/mL) was added to the apical side of ECs cultivated on inserts; after 1 hour of incubation, the material in the basolateral compartment was analyzed. A, The integrity of the translocated material isolated in the presence or absence of an endothelial monolayer was analyzed on an SDS–polyacrylamide gel. B, The particles isolated from the basolateral compartment in the presence or absence of an endothelial monolayer were analyzed by gel filtration and compared with lipid-free apoA-I. Elution profiles shown are representative of 3 independent experiments.

was 9.8 ± 0.03 nm in contrast to 10.6 ± 0.05 nm of the starting material or in contrast to 6.16 ± 0.1 nm for lipid-free apoA-I (Table I in the online data supplement). By contrast, HDL that was filtered through the cell-free porous membrane did not change its size (Online Table I).

The transport capacity of the cells was further investigated after adding the tracer into the apical chamber in the presence or absence of excess cold HDL at different concentrations. The specific transport was calculated by subtracting nonspecific transport from total transport (Figure 5A). The partial competition of ^{25}I-HDL transport through the cell layer suggests the occurrence of a specific transport. To further analyze the transport, the experiment was repeated at 4°C, a temperature that prevents internalization. The transport was almost abolished at this reduced temperature (Figure 5B), which supports the notion that HDL is transported transcellularly.

Identification of Proteins Modulating Transendothelial HDL Transport

To identify proteins that regulate HDL translocation, a candidate-based approach was chosen. SR-BI, ABCG1, and

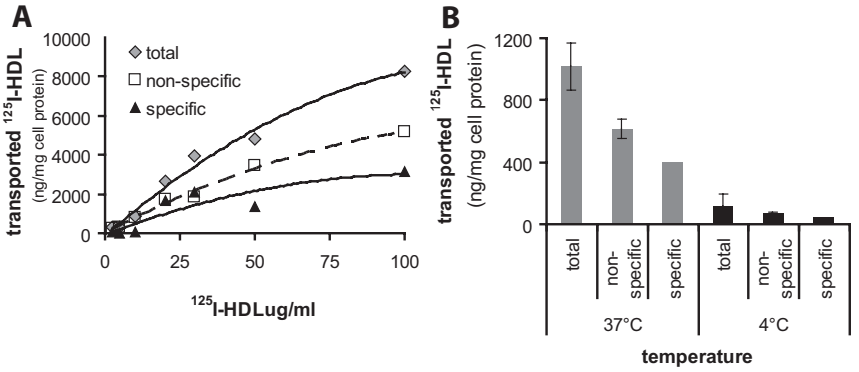

Figure 5. HDL transport through a monolayer of ECs is temperature-sensitive. A, ECs were cultured on inserts with the indicated concentration of ^{125}I-HDL in the absence (total) (◇) or presence of a 40-fold excess of unlabeled HDL (nonspecific) (□). Specific transport (▲) was calculated by subtracting the values of the unspecific from those of the total transport. B, ECs cultivated on inserts and incubated at 37°C and 4°C, respectively, with ^{125}I-HDL (added in the apical compartment) in the absence or presence of a 40-fold excess of unlabeled HDL. Specific transport was calculated as indicated above. The results are represented as means±SD of at least 3 individual experiments.

ABCA1 were considered as candidate receptors mediating binding, internalization, and, ultimately, the transport of HDL though ECs. All candidate genes are expressed in ECs. To evaluate their role in HDL binding, we suppressed SR-BI, ABCG1, and ABCA1 expression in ECs individually by the use of RNA interference. SR-BI, ABCA1, and ABCG1 transcriptions were reduced by 80% in cells transfected with SR-BI–, ABCA1-, and ABCG1-specific siRNA, respectively (Online Figure I). By contrast, no significant SR-BI mRNA reduction was observed in cells transfected with the ABCA1-specific siRNA, ABCG1-specific siRNA, or noncoding siRNA (Online Figure I). Similar results were observed for ABCA1- and ABCG1-specific silent cells (Online Figure I). On the protein level, the targeted protein expression was found significantly and specifically downregulated by each gene-specific siRNA (Figure 6A and 6B). The reduction on the protein level was less pronounced compared with corresponding mRNAs, probably because of the stability of the preformed protein.

Knock down of SR-BI reduced both cellular binding (4°C) and cell association (37°C) of HDL by 50% and 35% to 40%, respectively (Figure 6C and 6D). Suppression of ABCG1 reduced both cellular binding and association of HDL by 35% and 35% to 40% (Figure 6C and 6D). Interestingly the partial competition of ^{125}I-HDL binding by LDL (Figure 1C) was completely lost in the SR-BI knockdown cells but not in the ABCG1 knockdown cells, suggesting that SR-BI but not ABCG1 binds LDL in addition to HDL (Figure 6E). Interestingly, and in contrast to SR-BI or ABCG1 silencing, suppression of ABCA1 did not significantly reduce HDL binding and association by ECs. However, the binding of apoA-I (the typical interacting partner of ABCA1) was significantly reduced when ABCA1 expression was diminished (data not shown).[9] Thus, the role of ABCA1 in HDL cell internalization or HDL transport was not further studied. We next investigated the participation of SR-BI and ABCG1 in HDL internalization. After diminishing SR-BI or ABCG1 expression, the internalization of HDL was similarly reduced by approximately 40% to 45%, respectively, as compared to control (Figure 7E). We reproduced all findings described above by using additional sets of siRNAs (Online Figure II).

The finding that both SR-BI and ABCG1 participate in HDL cell binding, association, and internalization prompted

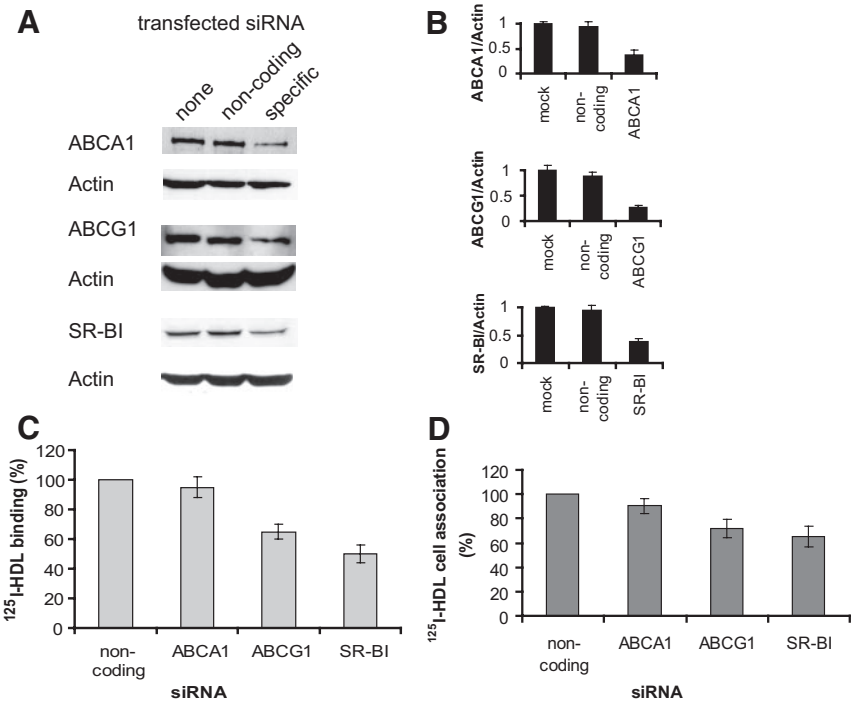

Figure 6. Role of SR-BI, ABCG1, and ABCA1 in HDL binding and cell association. To reduce SR-BI, ABCG1, and ABCA1 expression, specific siRNA were transfected. A, The protein levels were evaluated by Western blotting 72 hours after transfection. B, Quantification of protein expression levels is normalized to actin expression. First, specific HDL binding (C) at 4°C was measured after reducing the expression of SR-BI, ABCG1, and ABCA1 by RNA interference. D, Second, specific cell association was determined in cells after silencing the indicated genes.

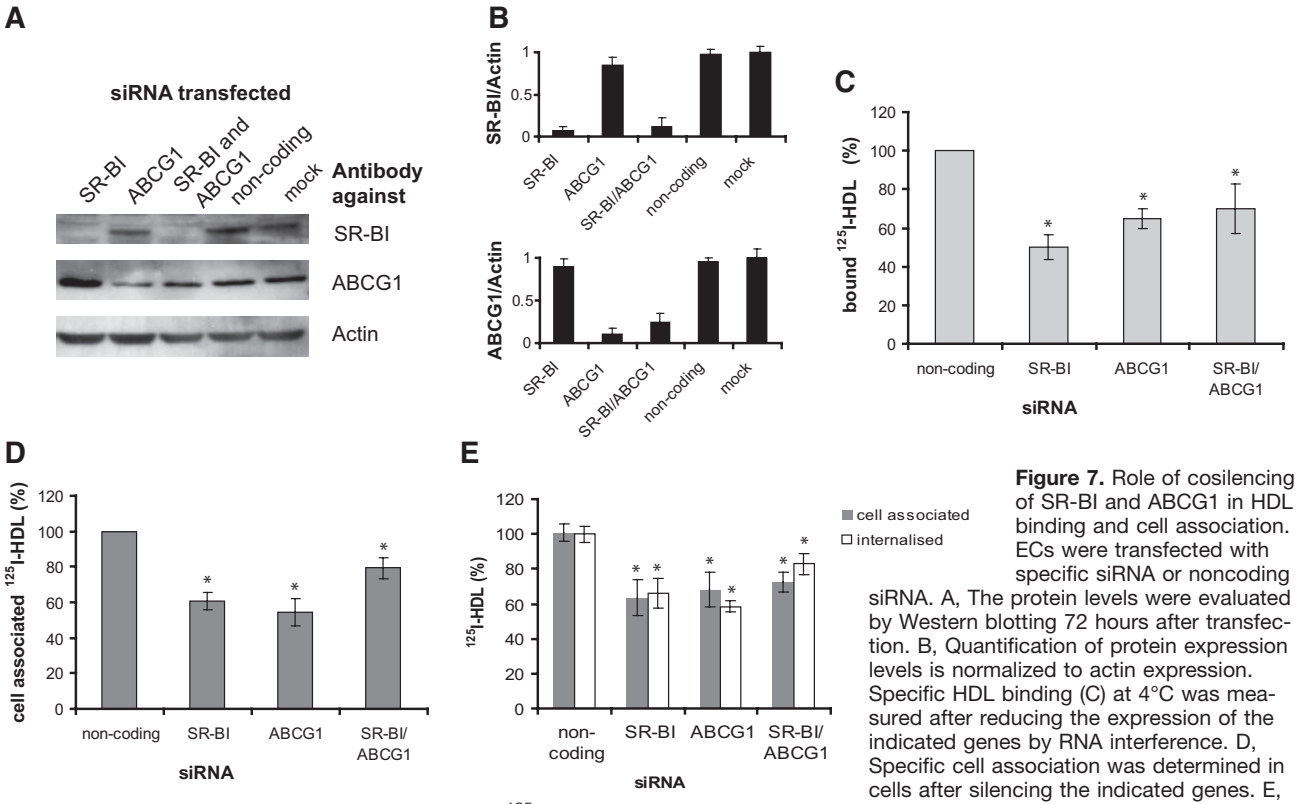

Figure 7. Role of cosilencing of SR-BI and ABCG1 in HDL binding and cell association. ECs were transfected with specific siRNA or noncoding siRNA. A, The protein levels were evaluated by Western blotting 72 hours after transfection. B, Quantification of protein expression levels is normalized to actin expression. Specific HDL binding (C) at 4°C was measured after reducing the expression of the indicated genes by RNA interference. D, Specific cell association was determined in cells after silencing the indicated genes. E, In independent experiments, the cells incubated with ^{125}I-HDL at 37°C were cell surface biotinylated to analyze the cellular distribution of HDL. The results are represented as means±SD of at least 3 individual experiments. *$P<0.05$ vs cells transfected with noncoding siRNA. Blots shown and quantified are representative of 2 independent experiments.

us to cotransfect the cells with siRNAs against both genes simultaneously. Cosuppression of SR-BI and ABCG1 with specific siRNA resulted in a reduced expression of both genes by 80% on the RNA level (Online Figure I). The protein expression levels of both genes were significantly reduced, as assessed by Western blotting (Figure 7A and 7B). HDL binding and association with SR-BI and ABCG1 cosuppressed cells were reduced by ≈30%, ie, to a similar degree as found in cells with only ABCG1 knockdown (Figure 7C and 7D). In the cotransfected cells, the internalization was reduced by 20% (Figure 7E). In general, the cotransfected cells revealed large variations both within and between experiments.

Finally, the implication of SR-BI and ABCG1 in HDL transport through the ECs was analyzed. HDL transport was reduced by 35% to 40% and 50% after silencing SR-BI or ABCG1, respectively (Figure 8A). Interestingly, whereas silencing of SR-BI had a stronger impact on HDL binding, ABCG1 knockdown had a more pronounced effect in HDL transport. Cosuppression of both genes together reduced transendothelial HDL transport by 30%, ie, to a similar extent as found in cells with a single knockdown of either SR-BI or ABCG1. Moreover, the integrity of the monolayer was verified after the specific siRNA treatment by analyzing the permeability of ^{3}H-inulin (Figure 8B). The permeability values for all transfected cells were similar, namely 2.97×10^{-5}, 2.90×10^{-5}, and 2.69×10^{-5} cm/sec for EC layers with knock downs of SR-BI, ABCG1, and SR-BI+ABCG1, respectively. These numbers are not significantly higher than in control (ie, 2.61×10^{-5} cm/sec). Addi-

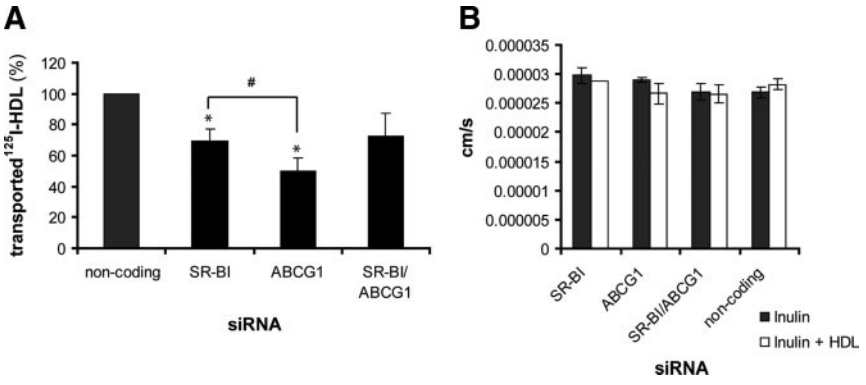

Figure 8. Role of SR-BI, ABCG1, and SR-BI/ABCG1 in HDL transport. Twenty-four hours after transfecting ECs with specific siRNA, or noncoding siRNA, the cells were cultivated on inserts, for 48 hours (A), then the specific transport from the apical to the basolateral compartment was analyzed as described above. B, The permeability of the cell layer to inulin was determined. The results are represented as means±SD of at least 3 individual experiments. *$P<0.05$ vs control (noncoding); #$P<0.05$ vs SR-BI silenced cells.

tion of 30 μg/mL HDL slightly reduced the permeability coefficients of ^{3}H-inulin to values of 2.88×10^{-5}, 2.67×10^{-5}, and 2.66×10^{-5} cm/sec. Also, these values are not significantly different from the permeability coefficients of ^{3}H-inulin alone (Figure 8B). This indicates that the transcellular HDL translocation is modulated by both SR-BI and ABCG1.

Discussion

In general, transendothelial transport of proteins occurs by paracellular and transcellular pathways. We have previously demonstrated that aortic ECs bind, internalize, and resecrete apoA-I in a competed and temperature-dependent manner.[9,10] Furthermore, we demonstrated that ABCA1 but not SR-BI modulates this process.[9] In the present study, we extend these findings by showing that ECs also bind, internalize, and transport mature HDL, however, by characteristics that are distinct from those of transendothelial apoA-I transport. Most importantly, SR-BI and ABCG1 but not ABCA1 are rate-limiting for HDL transport.

The presence of different pathways for the transendothelial transport of apoA-I and HDL parallels the need of at least 2 distinct molecules interacting with cells of the arterial wall and other extravascular compartments. Lipid-free apoA-I dissociates from mature HDL as a result of HDL remodeling by lipid transfer proteins and lipases.[12–14] Lipid-free apoA-I is important to mediate lipid efflux from macrophage foam cells via the ABCA1 pathway.[15] Although this lipid-efflux pathway generates a ligand for ABCG1-mediated lipid efflux, there appears to be additional need for preformed cholesterol acceptors, namely HDL.[16] In addition, after lipid loading of HDL from macrophage foam cells, it must leave the intimal space into the blood stream to deliver the acquired lipids to the liver. Also, this step requires the passage through the endothelium.

Consistent with previously published data,[17,18] we showed here that ECs specifically bind and associate HDL. Nonspecific binding of HDL to the cell surface can be ruled out because HDL binding was not competed by apolipoprotein-free liposomes but by apoA-I–containing liposomes, suggesting that HDL binding to ECs is protein-mediated (Figure 1D). Interestingly, HDL binding and association are not competed by apoA-I, whereas HDL competes for apoA-I binding and association. At first sight, these contradictory findings are well supported by the fact that lipid-free apoA-I is a poor ligand for SR-BI and ABCG1.[15,19] Furthermore, structural analysis of lipid-free apoA-I and apoA-I in HDL particles revealed different folding patterns[20] and consequently different functional domains. The partial competition of HDL binding and association by LDL can be explained by the involvement of SR-BI in HDL binding because LDL is also a ligand of this receptor, although with lower affinity than HDL.[21] This is further supported by the failure of LDL to compete for HDL binding in SR-BI knockdown cells (Figure 6E).

Interestingly, the binding of HDL to the polarized ECs appears to specifically occur on the apical site of the cells, which is in good agreement with our postulated transport of HDL from the blood into the arterial wall. Because the cells are cultivated on a membrane, one could argue that binding of HDL to the basolateral site is spatially hindered. However, the diffusion of inulin from the apical to basolateral and the basolateral to apical site did not differ significantly, arguing against spatial hindrance. However, the specific binding of HDL to the apical site of aortic ECs raises the question on how HDL particles leave the arterial wall after they have been loaded with cholesterol to complete reverse cholesterol transport. This process likely occurs via vasa vasorum, which grow from the adventitia into the thickening intima. ECs of these microvessels may well differ in their HDL-binding properties from ECs of the macrovasculature such as aorta, which have been used in our experiments.

By both cell surface biotinylation and fluorescent microscopy, we demonstrated that ECs internalize HDL. Like Wüstner et al,[22] in hepatocytes, we found FITC-labeled HDL partially colocalized with Alexa 594-conjugated transferrin. However, it is important to note that not all cells internalize HDL, even if they express ABCG1 and SR-BI.[16] For example, we have previously demonstrated that cholesterol efflux from RAW macrophages is coupled with internalization of apoA-I but not HDL. Importantly, the majority of the HDL internalized by ECs is not degraded but resecreted as intact proteins.

Because of the cytotoxicity of vesicular transport inhibitors such as *N*-ethylenimide, filipin, or dansylcadaverine, it was not possible to further study the nature of HDL translocation. For lipid-free apoA-I, we demonstrated by the use of siRNA technology that ABCA1 is a rate-limiting factor in the transport through ECs.[9] Therefore, we also used siRNA to analyze which proteins are mediating the specific interactions of HDL with ECs. In agreement with others,[23–25] we found that the best candidates were SR-BI, ABCA1, and ABCG1 expressed in ECs of bovine and human origin.[26] Their expression was successfully diminished by RNA interference (Figure 5A). As previously published, reduction of ABCA1 expression reduced neither HDL binding nor cell association because lipid-free apoA-I, rather than lipidated apoA-I or HDL, interacts with this transporter.[9] Knock down of both SR-BI and ABCG1 had a significant inhibitory effect on HDL-binding cell association and internalization. In addition, the transport of HDL was significantly impaired by suppression of either SR-BI or ABCG1. Interestingly, the transport in ABCG1-diminished cells was even more impaired than by knock down of SR-BI (Figure 8A). These differences may reflect that SR-BI, which is known to bind HDL by protein–protein interactions,[27] is a receptor in the proper sense, whereas ABCG1 is a lipid transporter for which the direct protein–protein interaction with HDL has not been proven. It is possible that ABCG1 only indirectly mediates cellular HDL binding by rearranging lipid domains in the plasma membranes that interact with HDL. This is in agreement with a recent publication by Terasaka et al[26] describing a nonredundant role of ABCG1 for the regulation of endothelium-dependent vasoreactivity in mice fed a high-cholesterol diet.

The stronger inhibitory effect of SR-BI knockdown on HDL binding than on internalization or transport may reflect that this receptor mediates fluxes of lipids from HDL into cells or from cells to HDL without holoparticle uptake and may explain the reduced particles size of the transported

material. However, it is also important to highlight that the siRNA approach used cannot distinguish SR-BI from its splice variant SR-BII, which has been described as an endocytic receptor.[28] The lower impact of SR-BI knockdown on HDL cell association and transport than binding indicates that HDL binding on the cell surface is a rate-limiting step in the transendothelial transport of HDL but also the coexistence of downstream effectors of this transport. In fact, the interaction of HDL with SR-BI was previously shown to promote endothelial repair by entailing several intracellular G protein–coupled signaling pathways, such as activation of src, phosphatidylinositol 3-kinase, or mitogen-activated protein kinases.[29] It is therefore tempting to speculate that one or several of these SR-BI mediated signaling pathways modulate endocytosis and intracellular transport of HDL (ie, transendothelial transport of HDL). In this regard, it is important to mention that HDL and sphingosine-1-phosphate, which in plasma is predominantly carried by HDL, as well as SR-BI, were previously shown to elicit several signaling effects in ECs,[30,31] which favor closure of interendothelial junctions and hence restrict the paracellular pathway of transendothelial transport.[32–35]

As yet, ABCG1 is only known as an important regulator of lipid efflux from macrophages to HDL. However, Terasaka et al[26] reported previously that ABCG1, unlike ABCA1, regulates the activity of endothelial nitric oxide synthase and thereby endothelium-dependent vasorelaxation in mice. The authors provided evidence that this regulatory effect of ABCG1 on nitric oxide production involves cholesterol and oxysterol efflux. Our data show that ABCG1 in ECs participates in HDL internalization and transport (Figures 7 and 8). Furthermore, the lower impact of ABCG1 suppression on HDL binding than on HDL internalization and transport supports the concept that ABCG1 does not directly bind HDL (Figure 6). Also, in the context of the work of Terasaka et al,[26] this suggests that ABCG1 modifies the lipid distribution of the plasma membrane and thereby the organization of integral plasma membrane proteins including those involved in endocytosis, such as caveolin or clathrin.

The finding that both SR-BI and ABCG1 participate in HDL binding and cell association prompted us to silence both genes simultaneously to determine whether the 2 proteins interact cooperatively or independently in the binding, internalization, and transport of HDL. Interestingly, the cosuppression of SR-BI and ABCG1 did not decrease HDL binding and cell association more severely than the single knockdowns, although on both the mRNA and protein level, the joint knockdowns were equally as efficient as the single knockdowns. Thus, it appears that SR-BI and ABCG1 cooperate in the modulation of HDL transport rather than act in parallel.

In summary, aortic ECs cultured on porous inserts bind, internalize, and translocate HDL particles from the apical to the basolateral compartment in a specific and temperature-dependent manner, without degrading the protein moiety but reducing the size of the particle. This process is modulated by SR-BI and ABCG1, but not ABCA1, which was previously found to modulate apoA-I transcytosis. Further studies are needed to evaluate the precise function of the identified proteins.

Acknowledgments

We thank Silvija Radosavljevic for technical assistance.

Sources of Funding

This work is supported by grants from the Swiss National Research Foundation (3100A0-100693/1 and 3100A0-116404/1), as well as by the European Union (LSHM-C-2006-037631).

Disclosures

None.

References

1. Curtiss LK, Valenta DT, Hime NJ, Rye KA. What is so special about apolipoprotein AI in reverse cholesterol transport? *Arterioscler Thromb Vasc Biol*. 2006;26:12–19.
2. Gordon DJ, Rifkind BM. High-density lipoprotein–the clinical implications of recent studies. *N Engl J Med*. 1989;321:1311–1316.
3. Tall AR, Yvan-Charvet L, Terasaka N, Pagler T, Wang N. HDL, ABC transporters, and cholesterol efflux: implications for the treatment of atherosclerosis. *Cell Metab*. 2008;7:365–375.
4. Rader DJ. Molecular regulation of HDL metabolism and function: implications for novel therapies. *J Clin Invest*. 2006;116:3090–3100.
5. Von Eckardstein A, Rohrer L. Transendothelial lipoprotein transport and regulation of endothelial permeability and integrity by lipoproteins. *Curr Opin Lipidol.* In press.
6. Vandenbroucke E, Mehta D, Minshall R, Malik AB. Regulation of endothelial junctional permeability. *Ann N Y Acad Sci*. 2008;1123:134–145.
7. Minshall RD, Malik AB. Transport across the endothelium: regulation of endothelial permeability. *Handb Exp Pharmacol.* 2006(176 p t 1):107–44.
8. Minshall RD, Tiruppathi C, Vogel SM, Malik AB. Vesicle formation and trafficking in endothelial cells and regulation of endothelial barrier function. *Histochem Cell Biol*. 2002;117:105–112.
9. Cavelier C, Rohrer L, von Eckardstein A. ATP-Binding cassette transporter A1 modulates apolipoprotein A-I transcytosis through aortic endothelial cells. *Circ Res*. 2006;99:1060–1066.
10. Rohrer L, Cavelier C, Fuchs S, Schluter MA, Volker W, von Eckardstein A. Binding, internalization and transport of apolipoprotein A-I by vascular endothelial cells. *Biochim Biophys Acta*. 2006;1761:186–194.
11. Freeman M, Ekkel Y, Rohrer L, Penman M, Freedman NJ, Chisolm GM, Krieger M. Expression of type I and type II bovine scavenger receptors in Chinese hamster ovary cells: lipid droplet accumulation and nonreciprocal cross competition by acetylated and oxidized low density lipoprotein. *Proc Natl Acad Sci U S A*. 1991;88:4931–4935.
12. Kunitake ST, Mendel CM, Hennessy LK. Interconversion between apolipoprotein A-I-containing lipoproteins of pre-beta and alpha electrophoretic mobilities. *J Lipid Res*. 1992;33:1807–1816.
13. Liang HQ, Rye KA, Barter PJ. Cycling of apolipoprotein A-I between lipid-associated and lipid-free pools. *Biochim Biophys Acta*. 1995;1257:31–37.
14. Liang HQ, Rye KA, Barter PJ. Dissociation of lipid-free apolipoprotein A-I from high density lipoproteins. *J Lipid Res*. 1994;35:1187–1199.
15. Lorenzi I, von Eckardstein A, Radosavljevic S, Rohrer L. Lipidation of apolipoprotein A-I by ATP-binding cassette transporter (ABC) A1 generates an interaction partner for ABCG1 but not for scavenger receptor BI. *Biochim Biophys Acta*. 2008;1781:306–313.
16. Lorenzi I, von Eckardstein A, Cavelier C, Radosavljevic S, Rohrer L. Apolipoprotein A-I but not high-density lipoproteins are internalised by RAW macrophages: roles of ATP-binding cassette transporter A1 and scavenger receptor BI. *J Mol Med*. 2008;86:171–183.
17. von Eckardstein A, Hersberger M, Rohrer L. Current understanding of the metabolism and biological actions of HDL. *Curr Opin Clin Nutr Metab Care*. 2005;8:147–152.
18. Mineo C, Deguchi H, Griffin JH, Shaul PW. Endothelial and antithrombotic actions of HDL. *Circ Res*. 2006;98:1352–1364.
19. Zannis VI, Chroni A, Krieger M. Role of apoA-I, ABCA1, LCAT, and SR-BI in the biogenesis of HDL. *J Mol Med*. 2006;84:276–294.
20. Davidson WS, Thompson TB. The structure of apolipoprotein A-I in high density lipoproteins. *J Biol Chem*. 2007;282:22249–22253.

21. Krieger M. Charting the fate of the "good cholesterol": identification and characterization of the high-density lipoprotein receptor SR-BI. *Annu Rev Biochem*. 1999;68:523–558.
22. Wüstner D. Mathematical analysis of hepatic high density lipoprotein transport based on quantitative imaging data. *J Biol Chem*. 2005;280:6766–6779.
23. Hatzopoulos AK, Rigotti A, Rosenberg RD, Krieger M. Temporal and spatial pattern of expression of the HDL receptor SR-BI during murine embryogenesis. *J Lipid Res*. 1998;39:495–508.
24. Brewer HB Jr, Remaley AT, Neufeld EB, Basso F, Joyce C. Regulation of plasma high-density lipoprotein levels by the ABCA1 transporter and the emerging role of high-density lipoprotein in the treatment of cardiovascular disease. *Arterioscler Thromb Vasc Biol*. 2004;24:1755–1760.
25. Hoekstra M, Kruijt JK, Van Eck M, Van Berkel TJ. Specific gene expression of ATP-binding cassette transporters and nuclear hormone receptors in rat liver parenchymal, endothelial, and Kupffer cells. *J Biol Chem*. 2003;278:25448–25453.
26. Terasaka N, Yu S, Yvan-Charvet L, Wang N, Mzhavia N, Langlois R, Pagler T, Li R, Welch CL, Goldberg IJ, Tall AR. ABCG1 and HDL protect against endothelial dysfunction in mice fed a high-cholesterol diet. *J Clin Invest*. 2008;118:3701–3713.
27. Acton S, Rigotti A, Landschulz KT, Xu S, Hobbs HH, Krieger M. Identification of scavenger receptor SR-BI as a high density lipoprotein receptor. *Science*. 1996;271:518–520.
28. Eckhardt ER, Cai L, Shetty S, Zhao Z, Szanto A, Webb NR, Van der Westhuyzen DR. High density lipoprotein endocytosis by scavenger receptor SR-BII is clathrin-dependent and requires a carboxyl-terminal dileucine motif. *J Biol Chem*. 2006;281:4348–4353.
29. Mineo C, Shaul PW. Role of high-density lipoprotein and scavenger receptor B type I in the promotion of endothelial repair. *Trends Cardiovasc Med*. 2007;17:156–161.
30. Argraves KM, Gazzolo PJ, Groh EM, Wilkerson BA, Matsuura BS, Twal WO, Hammad SM, Argraves WS. High density lipoprotein-associated sphingosine 1-phosphate promotes endothelial barrier function. *J Biol Chem*. 2008;283:25074–25081.
31. Argraves KM, Argraves WS. HDL serves as a S1P signaling platform mediating a multitude of cardiovascular effects. *J Lipid Res*. 2007;48:2325–2333.
32. Komarova YA, Mehta D, Malik AB. Dual regulation of endothelial junctional permeability. *Sci STKE*. 2007;2007:re8.
33. Mehta D, Malik AB. Signaling mechanisms regulating endothelial permeability. *Physiol Rev*. 2006;86:279–367.
34. Abdulla J, Haarbo J, Kober L, Torp-Pedersen C. Impact of implantable defibrillators and resynchronization therapy on outcome in patients with left ventricular dysfunction–a meta-analysis. *Cardiology*. 2006;106:249–255.
35. Zhu W, Saddar S, Seetharam D, Chambliss KL, Longoria C, Silver DL, Yuhanna IS, Shaul PW, Mineo C. The scavenger receptor class B type I adaptor protein PDZK1 maintains endothelial monolayer integrity. *Circ Res*. 2008;102:480–487.

Circulation Research
JOURNAL OF THE AMERICAN HEART ASSOCIATION

High-Density Lipoprotein Transport Through Aortic Endothelial Cells Involves Scavenger Receptor BI and ATP-Binding Cassette Transporter G1

Lucia Rohrer, Pascale M. Ohnsorg, Marc Lehner, Franziska Landolt, Franz Rinninger and Arnold von Eckardstein

Circ Res. 2009;104:1142-1150; originally published online April 16, 2009;
doi: 10.1161/CIRCRESAHA.108.190587
Circulation Research is published by the American Heart Association, 7272 Greenville Avenue, Dallas, TX 75231

Print ISSN: 0009-7330. Online ISSN: 1524-4571

Supplement Material

Materials and Methods

Phospholipid Liposome Preparation

Phospholipid liposomes were prepared containing 1,2-Diacyl-sn-glycero-3-phospho-L-serine (PS; Sigma) , phosphatidylcholine from egg yolk (PC; Sigma), and free cholesterol (C; Sigma) in the indicated molar ratios. The lipids were solubilized in chloroform and dried in a nitrogen stream. The dried lipids were resuspended in 150 mM NaCl, 0.1 mM EDTA, 10 mM HEPES, pH 7.5. Once the samples were fully hydrated, they were extruded through 0.1-µm pore size polycarbonate membranes using a mini-extruder device (Avanti Polar Lipids). After extrusion, liposomes were dialyzed against 150 mM NaCl, 0.1 mM EDTA, pH 7.5, sterile filtrated and then stored under nitrogen at 4 °C [1]. In the competition experiments the phospholipid concentration in the assay was 400 µg/ml. Based on an average phospholipid mass of 785 g/mol, a liposome concentration of 400 µg phospholipid/ml converts to 4.8 nM in liposome particles.

^{125}I-HDL Binding, Cell Association, and Degradation Assays

Binding, cell association, and degradation assays were performed as previously described for ^{125}I-apoA-I[2] . In brief ECs were seeded into 12-well dishes at a concentration of $3x10^5$ cells/well for HDL binding and internalisation studies or in 24-well dishes at a concentration of $1x10^5$ cells/well for HDL cell association and degradation experiments. The assays were performed in DMEM/25 mM Hepes/0.2% BSA (medium C) containing 10 µg/ml ^{125}I-HDL (or the indicated amount), in the absence (total binding) or in the presence (non-specific binding) of a 40-fold excess of unlabelled HDL (or the indicated competitor). After incubation, the amounts of cell associated radioactivity were determined using a Perkin Elmer γ-counter and the protein content was analyzed as described previously [2]. Specific cell association or binding were determined by subtracting the values obtained in the presence of the excess unlabelled HDL (nonspecific) from those obtained in the absence of the unlabelled HDL

(total). For differential binding studies in ECs cultured in a two compartment system, ECs were seeded in cell culture inserts ($1x10^5$ cells/insert) and cultivated for 3 days to form a tight monolayer. The binding and cell association experiments were performed as described [2]. Degradation of ^{125}I -HDL by ECs was measured as described previously [2].

Internalisation assay

The internalisation assay was performed as described[2]. In brief, after incubation with 10 μg/ml ^{125}I -HDL in medium C at 37°C, the cell surface proteins were biotinylated at 4°C using NHS-biotin (Pierce). The streptavidin beads with the bound cell surface proteins were removed from the supernatant that contained the not biotinylated and consequently internalized protein. The radioactivity in the supernatant was measured in a Perkin Elmer γ-counter.

Confocal fluorescence microscopy

Cells were incubated 30 minutes with 10 μg/mL HDL labelled with FITC, and 5 μg/mL alexa596 transferrin washed 6 times 5 min in PBS, fixed in 3% paraformaldehyde for 10 min. Confocal microscopy was performed with a 63x oil-immersion lens in the sequential mode.

Transport studies

The transport studies were performed as previously described for apoA-I [2]. Before determining the transport direction, the tightness of the endothelial cell monolayer was assessed by measuring the permeability of ^{3}H-inulin. Permeability calculations were performed using an equation which was derived from Fick's first law and described by Youdim et al. [3]:

The HDL transport studies were performed in medium C and ^{125}I -HDL was added to the upper chamber without (quadruple determinations) and with a 40-fold excess of unlabelled HDL at the indicated final concentrations (double determinations). The radioactivity was

directly measured and the protein bound radioactivity was calculated as the difference of total radioactivity minus non-trichloroacetic acid (TCA) precipitable radioactivity. Furthermore, the proteins of the translocated ^{125}I -HDL were analyzed for their integrity by electrophoresis in 10% SDS gels. The gel was exposed after fixation to a phosphor imager screen.

siRNA transfection

EC were transfected with 30 nM BLOCK-iT^{TM} fluorescent oligo and 100 nM Stealth siRNA (Invitrogen) or 100nM siRNA siGenome ON-TARGETplus SMARTpool duplex (Dharmacon) against either SR-BI: 507 (TCGTCATGCCCAACATCCTGGTCTT) and 1275 (CCACCACAG TGTTGCTTGACAGCTT), ABCA1: (GGGACTTAGTGGGACGAAATCTCTT), ABCG1: 504 (CGTCCTGCTCTTCTCCGGATTCTT), or D5 (AAGTACAGCAGGCCAATGATT, AATGTG CGAGGTGATGCGCTT, TATCTCCTTGACCATTTCCTT, TTTCAGGAGGGTCTTGTATTT) (Dharmacon) or scrambled (noncoding) W1(AGAGCTTATCCCTCGGTTGTGTCGT) and standard siCONTROL reagents (D1) (Dharmacon) with Lipofectamine 2000 (Invitrogen) in OPTIMEM according to the manufacturer's protocol. 6 h after transfection, the medium was replaced by DMEM 5% FCS. Binding, internalisation, and transport assays were conducted between 60 and 72 h after transfection. The efficiency of the silencing was evaluated by quantitative RT-PCR and Western-blotting.

Quantitative RT-PCR

Total RNA was isolated from cells using Tri Reagent according to the manufacturer's instructions (Molecular Research Center, Cincinnati, USA). Reverse transcription was performed using Superscript II RT (Invitrogen) and following the standard procedure as defined by the manufacturer. Quantitative PCR was done with LightCycler FastStart DNA Master SYBR Green I (Roche). Gene specific primers were used as follows: ABCA1 (GTCATTATCATCTTCATCTGCTTCC, CCTCACATCTTCATCTTCATCATTC, 60°C, 5 mmol/L $MgCl_2$), SR-BI (GGAATCCCCATG AACTG, CTTGGGAGCTGATGTCATC, 58°C, 5

mmol/L $MgCl_2$), and ABCG1 (GGCCTACT GCAGCATCGTGT, TCTGGAAATGGCAGGTCTCG, 58°C, 5 mmol/L $MgCl_2$) transcription levels were normalized to GAPDH (GTCTTCACTACCATGGAGAAGG, TCATGGATGA CCTTGGCCAG, 58°C, 4 mmol/L $MgCl_2$). Data analysis was performed using the ΔΔCt method.

Western-blotting

EC were lysed in RIPA buffer (10 mmol/L Tris pH 7.4, 150 mmol/L NaCl, 1% NP-40, 1% sodium deoxycholate, 0.1% SDS, complete EDTA (Roche)). Equal amounts of total protein were separated on a SDS-PAGE and transblotted onto a PVDF membrane (GE Healthcare). The expression of ABCA1 (anti ABCA1 ab18180, Abcam, Cambridge, UK), ABCG1 (anti ABCG1 NB 400-132, Novus Biologicals, Littleton, USA) and SR-BI (anti SR-BI ab3, Abcam, Cambridge, UK) were evaluated and compared to the expression of actin (anti actin AC-15, Sigma).

^{125}I-HDL transport

Transport assays were performed as previously described [2, 4]. In brief, $1x10^5$ cells were seeded 2 days in advance on the upper side of porous membrane inserts (0.4 μm, BD Biosciences) precoated with collagen type I (BD Biosciences). The apical medium contained 30 μg/ml HDL and transport from the apical to the basolateral compartment was measured after 60 min or the indicated time period.

Gel filtration chromatography

The size of HDL and apoA-I before and after transport was analyzed by gel filtration chromatography as described [5]. In brief medium (0.3 ml) isolated from the basolateral compartment was loaded onto a Sephacryl S-200 HR column (60x1.6 cm) (GE-Healthcare) using an Akta fast-protein liquid chromatography (FPLC) system and eluted with Tris-buffered saline (10 mmol/L Tris, 150 mmol/L NaCl) plus EDTA, pH 7.5, at a flow rate of 1

ml/min. Fractions (1 ml) were collected and the amounts of transported radioactivity were determined using a Perkin Elmer γ-counter. The sizes of the lipid particles eluting in the various fractions were determined by comparing their K_{av} values with those of proteins with known diameters (particle diameter range of 6.1–17 nm). K_{av} was calculated using the following equation: $K_{av} = (V_e - V_0)/(V_t - V_0)$, where V_0 is the void volume, V_t is the total column volume, and Ve is the elution volume as described [5]. A plot of log particle size against K_{av} was constructed, and the points were fitted by linear regression analysis. The particle size (hydrodynamic diameter in nm) was calculated using the following equation: $\log_{10}$ diameter = $1.27 - 0.95\ K_{av}$.

Statistical Analyses

The data for all experiments were analyzed using GraphPad Prism 5 software program. Comparisons between groups were performed using t-test methods. Experiments were routinely performed in triplicates or quadruplets. The data have been obtained from 3-5 independent experiments, if not indicated otherwise and are graphically represented as means +/- SD.

Online Table I

The stokes' diameter of the translocated material were determined.

	particles diameter (nm)
ApoA-I	6.16 +/- 0.1
HDL (starting material)	10.62 +/- 0.05
HDL no cell contact	10.64 +/- 0.05
HDL with cell contact	9.8 +/- 0.03

The results are represented as means +/- SD of at least three individual experiments.

References

1. Liu B, Krieger M. Highly purified scavenger receptor class B, type I reconstituted into phosphatidylcholine/cholesterol liposomes mediates high affinity high density lipoprotein binding and selective lipid uptake. *J Biol Chem.* 2002;277:34125-34135.

2. Rohrer L, Cavelier C, Fuchs S, Schluter MA, Volker W, von Eckardstein A. Binding, internalization and transport of apolipoprotein A-I by vascular endothelial cells. *Biochim Biophys Acta.* 2006;1761:186-194.

3. Youdim KA, Avdeef A, Abbott NJ. In vitro trans-monolayer permeability calculations: often forgotten assumptions. *Drug Discov Today.* 2003;8:997-1003.

4. Cavelier C, Lorenzi I, Rohrer L, von Eckardstein A. Lipid efflux by the ATP-binding cassette transporters ABCA1 and ABCG1. *Biochim Biophys Acta.* 2006;1761:655-666.

5. Liu L, Bortnick AE, Nickel M, Dhanasekaran P, Subbaiah PV, Lund-Katz S, Rothblat GH, Phillips MC. Effects of apolipoprotein A-I on ATP-binding cassette transporter A1-mediated efflux of macrophage phospholipid and cholesterol: formation of nascent high density lipoprotein particles. *J Biol Chem.* 2003;278:42976-42984.

Online Figure I

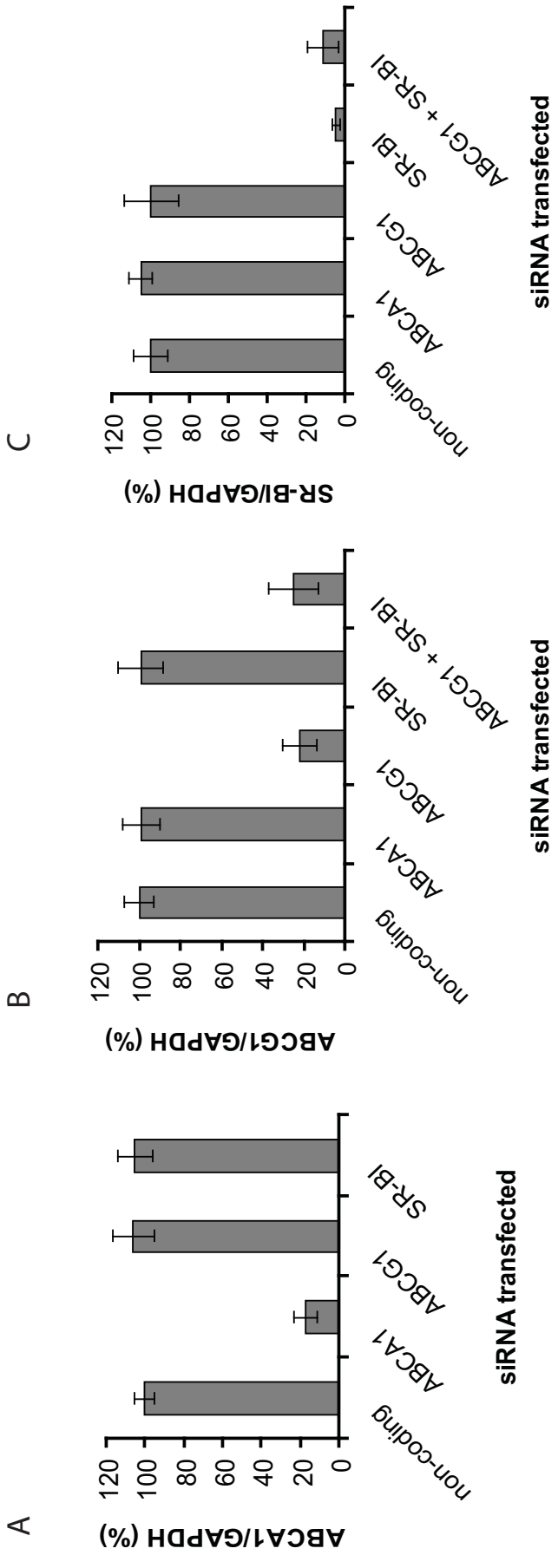

Online Figure II

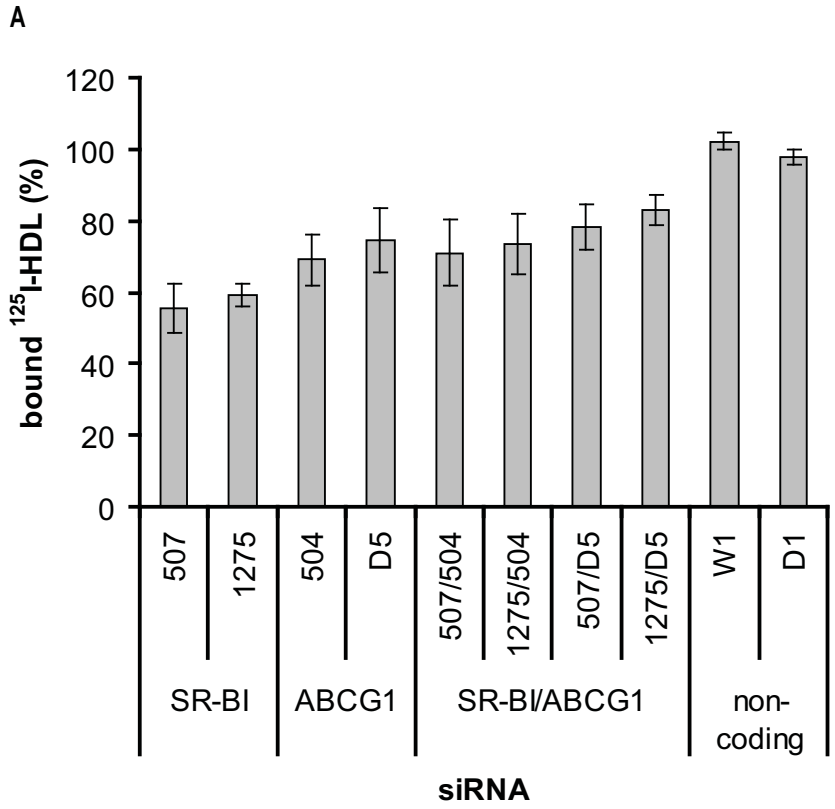

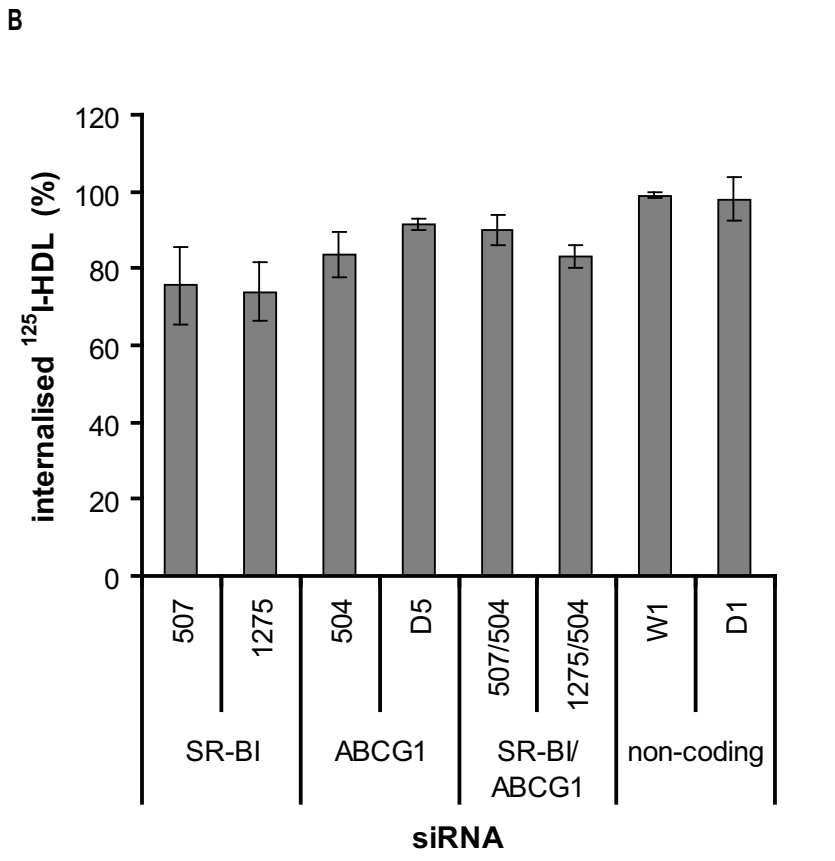

Figures

Online Figure I

Expression analysis of ABCA1, ABCG1, and SR-BI in siRNA transfected cells. In order to reduce SR-BI, ABCG1, and ABCA1 expression specific siRNAs were transfected. The RNA levels were evaluated by real time RT-PCR 72h after transfection. ABCA1expression levels (A), ABCG1 expression (B) and SR-BI expression levels (C) were determined in cells transfected with the indicated siRNA.

Online Figure II

Verification of SR-BI and ABCG1 involvement in HDL binding and internalisation. First, ECs were transfected with specific siRNA, or non-coding siRNA. (A) Specific HDL binding was measured after reducing the indicated genes by RNA interference 72h post transfection. (B) Second, specific HDL internalisation was determined in cells after silencing the indicated genes by cell surface biotinylation.